Magnetic order and electronic structure in thin films

1999 J. Phys.: Condens. Matter 11 9421

(http://iopscience.iop.org/0953-8984/11/48/306)

J. Phys.: Condens. Matter **11** (1999) 9421–9436. Printed in the UK PII: S0953-8984(99)07434-2

Magnetic order and electronic structure in thin films

Markus Donath

Max-Planck-Institut für Plasmaphysik, Euratom Association, Surface Physics Division, D-85740 Garching bei München, Germany

Received 2 September 1999

Abstract. The magnetic order in ultrathin films depends critically on a variety of film parameters. Therefore, to understand the magnetic properties of thin films on the basis of the spin-dependent electronic structure is a challenging task for both experimentalists and theoreticians. Experimentally, spin-resolved electron spectroscopies probe directly either the spin-dependent density of states or specific energy states, often at a defined wave vector. In this paper, two surface-sensitive techniques, that provide complementary information about the unoccupied electronic states, are described. Spin-resolved appearance potential spectroscopy gives element-specific access to the spin-dependent local density of states. Spin-resolved inverse photoemission permits detailed investigations of electron states characteristic of the surface and the layers underneath as a function of the wave vector. Both techniques are sensitive also to the film structure. A variety of magnetic film properties is discussed in the light of the electronic structure. The examples described in this paper include Fe films on W(110) and Cu(001) as well as Gd films on W(110).

1. Introduction

Few elemental systems exhibit collective magnetic order phenomena but a huge number of compound and alloy systems are magnets. Magnetism has attracted generations of scientists and still remains one of the great puzzles of solid state physics [1]. For a long time magnetism was considered a bulk problem. By alloying magnetic elements with other magnetic or nonmagnetic elements it became possible to tailor the magnetic properties for certain applications. The success of surface-science experiments under ultra-high-vacuum conditions in the last 20 years opened new horizons. The importance of interface effects became quickly apparent. Enhanced or reduced magnetic moments at surfaces and interfaces, enhanced Curie temperatures of the surface compared with the bulk, modified magnetic anisotropies, the influence of the growth mode, distorted crystal structures etc: all these topics have been the subject of numerous studies [2–7]. The discovery of the giant magnetoresistance effect in sandwich structures consisting of magnetic and nonmagnetic layers and its tremendous potential for applications in sensor and data storage technology motivated even more groups to start research in magnetism. The search for novel phenomena in more and more sophisticated multilayer structures as well as the development of magnetic microscopies with lateral resolution in the nanometre range are now beginning to dominate the field.

Nevertheless, the understanding of magnetic phenomena on the basis of the electronic structure still lags behind. Even today, there is no complete theory to describe the ferromagnetism of the classical band ferromagnets Fe, Co and Ni. This is even more true for low-dimensional layered structures. Experiments are needed that determine the spin-dependent electronic states and provide a data base for band-structure-based models that

0953-8984/99/489421+16$30.00

describe the magnetic phenomena. In this paper, the relation between the magnetic order and the electronic structure will be discussed with respect to three aspects: (i) the dependence on the film thickness and, connected with that, the influence of the growth characteristics, (ii) the dependence on the depth, i.e. the question of a magnetic depth profile, and (iii) the dependence on the temperature, which is the most fundamental dependence in magnetism. Two techniques, appearance potential spectroscopy (APS) and inverse photoemission (IPE), both in a spin-resolved mode, are described. As model systems, Fe on W(110) and Cu(001) as well as Gd on W(110) will be discussed.

2. Experiment

The experiments were performed in ultra-high-vacuum (UHV) chambers with base pressures of 3 to 5×10^{-9} Pa. The Cu(001) substrate was cleaned by Ar^+ or Ne^+ bombardment and subsequent annealing to about 1000 K. The W(110) substrate was cleaned by cycles of glowing at 1500 K in oxygen atmosphere (1 to 5×10^{-5} Pa) and subsequent flash desorption at 2500 K. Fe and Gd films were deposited from electron-beam evaporators. Fe was evaporated from a carefully outgassed 2 mm thick Fe rod (purity 99.999%) at a rate of $\approx$0.6 monolayers (ML) per minute. The Cu(001) substrate was kept at 300 K during evaporation [8–11]. For Fe on W(110), the sample was kept 300 K during evaporation of up to 6 ML and subsequently annealed at 350 K. For thicker films the sample temperature during evaporation was continuously increased up to 550 K after the sixth layer was deposited [12, 13]. This procedure leads to flat and well ordered Fe films with sharp LEED patterns. Gd (carefully outgassed, 99.9%) was evaporated from an Mo crucible at a rate of $\approx$13 Å min^{-1}. The W(110) substrate was kept at 320 K during evaporation and the films were subsequently annealed for 2 min [14, 15]. The annealing temperature was chosen depending on the film thickness according to the literature [16]. The pressure during evaporation was always below 3×10^{-8} Pa. The cleanness and structural order of the substrates and the deposited films were characterized by low-energy electron diffraction (LEED), Auger electron spectroscopy (AES) and APS or IPE (intensity of surface states). The coverages were determined by LEED, AES, a quartz microbalance and film-specific calibration marks, e.g. typical LEED patterns or structural and magnetic phase transitions. The adlayers were remanently magnetized by an external field either in the film plane or perpendicular to it. The magnetization was checked by the *in situ* magneto-optic Kerr effect (MOKE).

Both experiments consist of a two-chamber UHV system. One chamber contains the source for spin-polarized electrons, the other chamber the techniques for film preparation and characterization plus the detectors used for APS or IPE. An electron transfer system connects both chambers. The spin-polarized electrons are photoemitted from negative-electron-affinity (NEA) GaAs excited by circularly polarized laser light. In our geometry, we obtain a transversal spin polarization of about 30% [17–19]. Since the spin dependence of the measured signals is proportional to the scalar product of the electron spin polarization $\boldsymbol{P}$ and the sample magnetization $\boldsymbol{M}$, our experiment is sensitive to an in-plane film magnetization for normal electron incidence on the sample. In the APS apparatus we have included a spin rotator in our electron optics able to rotate the electron spin polarization within the transversal plane [13]. Here, we can monitor reorientation transitions, where the direction of easy magnetization changes in the film plane. Out-of-plane components are detectable for off-normal electron incidence. To eliminate the influence of the incomplete experimental beam polarization on the data, all spin-resolved spectra have been renormalized to 100% hypothetical beam polarization. The spin asymmetry of the measured signals is defined as the normalized difference between the signals $I_\uparrow$ and $I_\downarrow$ for electron excitation with spin magnetic moment parallel ($\uparrow$) and antiparallel ($\downarrow$) to the magnetization direction, respectively: $A = (I_\uparrow - I_\downarrow)/(I_\uparrow + I_\downarrow)$. Please note that in

some publications A is defined with the reversed sign to obtain positive numbers at energies above the Fermi level, where minority states dominate.

2.1. Spin-resolved appearance potential spectroscopy

For APS the surface of a solid is bombarded with electrons of variable energy while the total yield of emitted electrons or, as in our case, x-rays is monitored. At energies high enough to excite a core electron into states above the Fermi level E_F the yield of emitted particles increases owing to recombination of the created core hole via x-ray or Auger electron emission. The primary energy of the electrons used for excitation is given by $E_p = eU + \Phi_C$, where U denotes the potential between photocathode and sample and Φ_C the work function of the cathode. The relevant number of our negative-electron-affinity cathode was determined as 1.4 eV and represents essentially the band gap of the semiconductor. In the literature the scale for the electron energy is given by either the potential U, the electron energy eU or E_p as defined above. This explains the somewhat different energies of APS lines in the literature. The APS signal is detected via soft-x-ray emission in our experiment. The detector arrangement consists of a multichannel plate with filters and a CsI layer as transmission photocathode acting as photon-to-electron converter [20]. Due to the low signal-to-background ratio of typically 10^{-4} the APS signal is measured by modulating the sample potential and monitoring the first derivative with lock-in technique. The voltage for potential modulation is chosen in such a way that the observed APS line widths are not influenced, typically 1 to 2 V peak-to-peak. Electron beam currents range from 30 to 60 μA.

Since core electrons are involved in the excitation process, APS is element specific and therefore able to determine binding energies of core levels [21–23]. The intensity and shape of the APS signal reflect the density of unoccupied states because both the exciting and the excited electrons are scattered into unoccupied states. Within a one-particle approximation, the APS signal is proportional to a self-convolution of the local unoccupied DOS. As a consequence, APS can be used to investigate the unoccupied DOS [24, 25]. Since the shape of the DOS depends on the structure, APS is sensitive to the crystal structure [26] and to structural changes caused by melting [27], alloying [28] or at interfaces in films [13]. The surface sensitivity of APS is determined by the inelastic mean free path of the exciting electrons at the excitation energy, which is typically a few monolayers only. This limits the experimentalist's access to shallow buried interfaces or surfaces only. With spin resolution APS is able to reveal the spin dependence of the unoccupied DOS [29, 30, 28] as well as the sign of the magnetic coupling in multicomponent systems [31]. By taking into account matrix elements, but still within the one-particle approximation, it is possible to calculate the measured spin-resolved APS signals of 3d metals and alloys [32, 28]. By measuring the spin asymmetry as a function of the film thickness or the temperature, APS can be used for magnetometry measurements [8, 9, 33, 13].

2.2. Spin-resolved inverse photoemission

For IPE low-energy electrons impinge on the sample as a parallel beam. Radiative transitions between empty states are observed via the emitted photons. Angle-resolved IPE measures the energy versus wave vector relation $E(\boldsymbol{k})$ of unoccupied electronic states at surfaces [34, 35]. In our experiment, the photons are detected at a fixed energy in iodine-filled Geiger-Müller counters with SrF_2 as entrance windows [36]. This detector works as an energy bandpass detector around 9.4 eV. The apparatus function representing the overall experimental resolution including the energy spread of the electron beam is well described by a Gaussian function with a full width at half maximum (FWHM) of about 450 meV [19]. IPE spectra display the number

of detected photons as a function of the kinetic energy of the exciting electrons. Usually the energy scale gives the final state energies referenced to the Fermi level of the sample, which is the energy where the intensity onset appears. In magnetic systems the energy levels $E_{\uparrow,\downarrow}$ depend on the electron spin magnetic moment parallel ($\uparrow$) or antiparallel ($\downarrow$) to the magnetization direction. The energy difference between $E_{\uparrow}$ and $E_{\downarrow}$ is called the exchange splitting ΔE_{ex} which depends on the energy E, the wave vector $\boldsymbol{k}$ and the temperature T. With spin-polarized electrons used for excitation, the spin-split bands in magnetically ordered materials are determined directly [92, 38].

Experiments with IPE complement the results obtained with ordinary photoemission (PE) about the occupied valence bands. For understanding magnetic systems the states just below and above the Fermi energy are of particular importance. Connected with the exchange-split bands close to the Fermi energy E_F, i.e. the spin-dependent Fermi surface, is an imbalance in occupation of the spin-up (majority, $\uparrow$) and spin-down (minority, $\downarrow$) energy levels, which leads to a net magnetic moment. As a consequence, electronic states with spin-dependent occupation close to E_F contribute directly to the magnetic moment. To investigate these states as a function of film parameters and the temperature helps in the development of a microscopic picture of ferromagnetism. The information depth of IPE is, in general, determined by the inelastic mean free path for low-energy electrons, which is a few atomic layers only and spin-dependent [39, 40, 12]. However, the ability to select specific electronic states with defined $\boldsymbol{k}$ leads to an effective probing depth that depends on the specific state under investigation. Results of two-dimensional surface states, for example, carry information from the very first layer [41].

3. Thickness dependence

The magnetic order and the electronic structure depend critically on the film thickness. The Curie temperature, the magnetic moment per atom, the magnetic anisotropy and more properties are different in ultrathin films than in the bulk even if one assumes the same crystal structure as in the bulk. In addition, a modified lattice constant, structural phase transitions as a function of the thickness and interface effects influence the magnetic and electronic properties.

As a first example we discuss bcc-like Fe films grown on W(110). Despite the lattice mismatch of 9.4% between W and Fe, the first 1.8 ML forms a pseudomorphic overlayer. During the growth of further layers the tensile stress is continuously released by a dislocation network. Finally, at thicker films above 9 ML, the Fe bcc lattice constant is adopted. Details of the growth mode are published in the literature [42–45]. Here we present APS measurements of this thin-film system. Figure 1 shows spin-integrated APS measurements in the energy range of the Fe 2p threshold for different film thicknesses [13]. Compared with the spectrum for a 10 ML thick film, the thinner films exhibit a shift in energy, a modified ratio between the spin–orbit-split components (branching ratio) and the absence of a spectral feature at about 715 eV. The energy shift is due to interface effects, i.e. a core-level shift and a modified density of unoccupied d states, which may also account for the modified branching ratio [13]. The spectral feature at 715 eV results from a maximum of the sp-derived DOS at critical point energies [24]. The appearance of this feature with increasing film thickness demonstrates the development of the three-dimensional band structure. The dominant APS lines which reflect the DOS of the more localized d states are detected already in the submonolayer range. The delocalized sp states, however, need at least 4 ML for sufficient long-range order for the critical points in the Brillouin zone with an enhanced DOS to be observed. It might be interesting to note that angle-resolved IPE measurements (not shown here) are even more sensitive to a well defined $\boldsymbol{k}$ in the sample. The intensity of a direct, i.e. $\boldsymbol{k}$-conserving, transition into an empty

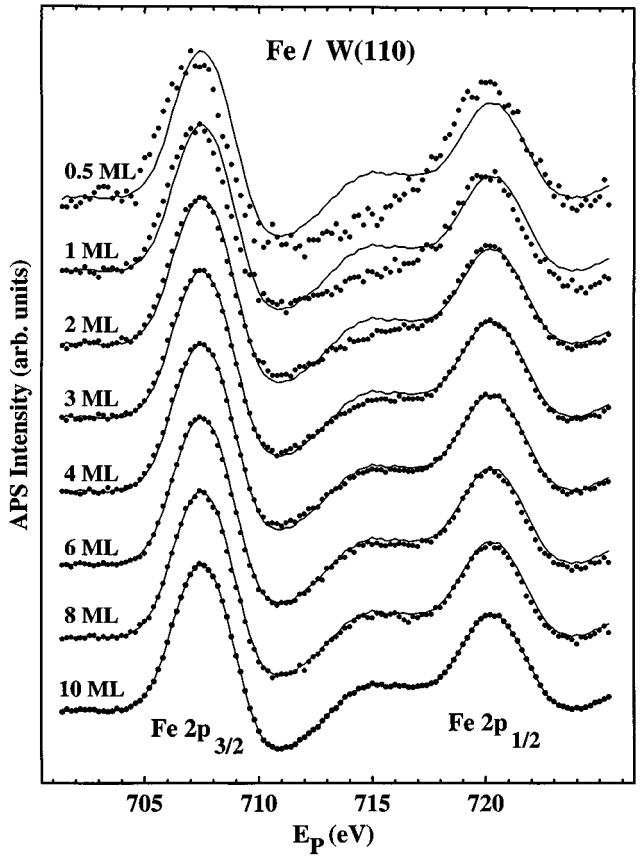

Figure 1. Spin-integrated APS spectra of the Fe 2p thresholds for Fe films on W(110). For comparison, the data for 10 ML are included as solid lines in the spectra for thinner films [13].

minority d state starts to develop at 3 ML Fe on W(110) and increases up to about 10 ML [12], which reflects the improving three-dimensional crystallographic order with increasing film thickness.

The magnetic properties of Fe films on W(110) were monitored via the spin asymmetry of the $2p_{3/2}$ line. The results are shown in figure 2 as a function of the Fe film thickness. For films thicker than about 45 ML the films are spontaneously magnetized along [001], which is the direction of easy magnetization in bulk bcc Fe. For thinner films, the magnetic anisotropy is influenced by the Fe/W interface leading to a direction of easy magnetization along $[1\bar{1}0]$ [46]. This magnetic reorientation transition with increasing thickness was followed by rotating the spin polarization of the incoming electron beam, whereas the absolute value of A of about 0.29 did not change as shown in figure 2. The low spin-asymmetry values for films thinner than 3 ML cannot be explained by a reduced T_C of the film. Our sample temperature was below the T_C values reported in the literature for these film thicknesses [47]. The suppression of asymmetry is presumably a result of an incomplete sample magnetization due to high in-plane coercivity in this thickness range [48]. Our external field was not high enough to saturate the very thin films. The asymmetry maximum around 6 ML came as a surprise. It cannot be explained by an enhanced magnetic moment of only the surface layer which is theoretically predicted [49, 50] and experimentally confirmed for Fe(110) [51–53]. The solid line in figure 2 simulates the

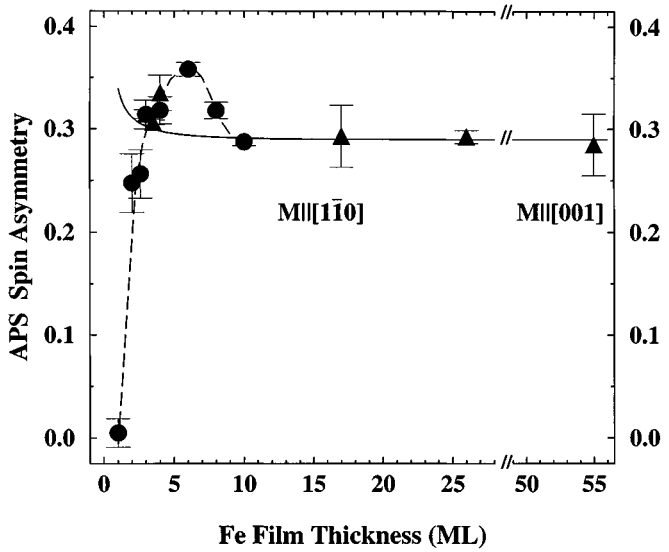

Figure 2. Spin asymmetry of the Fe $2p_{3/2}$ APS signal for Fe/W(110) as a function of the Fe film thickness at two different sample temperatures of 150 K (dots) and 300 K (triangles) [13].

influence of an enhanced surface magnetic moment by taking into account the probing depth of APS [13]. As a consequence, either the asymmetry maximum reflects an enhanced magnetic moment per atom in this thickness range, where the films have a complicated film morphology, or the enhanced asymmetry is due to peculiar modifications of the shape of the unoccupied DOS. The latter is unlikely because the spin-integrated APS line shape does not change as a function of the film thickness (see figure 1). Therefore, we attribute the enhanced asymmetry to enhanced magnetic moments due to the structural changes taking place at low coverages. The dislocation network leads to a continuous change of the lattice constant of the film and to an enhanced corrugation of the surface. Step atoms are known to have an enhanced magnetic moment even higher than surface atoms [53]. Moreover, an expanded lattice also tends to cause enhanced moments. Both effects may account for the asymmetry maximum observed for Fe thickness where the film has not reached the bulklike structure.

The second example is Fe on Cu(001), which is probably the most studied magnetic thin-film system in the literature [54–61]. When Fe is deposited on Cu(001) at room temperature it exhibits three phases. Up to 5 ML, the films have a tetragonally distorted fcc structure, they are ferromagnetic with out-of-plane anisotropy. Between 5 and 10 ML, the structure is fcc with a reconstructed surface, the out-of-plane ferromagnetic signal is reduced and independent of the film thickness. For more than 10 ML, a structural phase transition to bcc occurs and the magnetization direction changes to in plane. Most attention was given to the thickness range between 5 and 10 ML to understand the unexpected reduced magnetization. The results of several experiments favoured magnetically live surface layers on paramagnetic or antiferromagnetic Fe sublayers.

Figure 3 displays spin-integrated APS spectra for three thicknesses of Fe on Cu(001) representative of the three phases described above [8]. For 17 ML the APS spectrum resembles the typical spectra for bcc Fe on W(110) as shown in figure 1. For 3 and 6 ML, the spectral feature between 710 and 715 eV has changed and looks like that in earlier APS measurements for γ-Fe at temperatures between 1184 and 1673 K with fcc crystal structure [62]. The

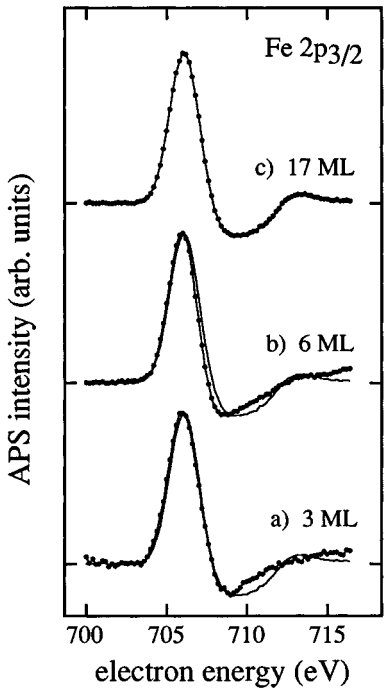

Figure 3. Spin-integrated APS spectra of the Fe $2p_{3/2}$ core level for Fe films on Cu(001) taken at three different coverages. Thin solid line: spectrum of 17 ML Fe/Cu(001) [8].

described spectral feature serves as a fingerprint to distinguish between different crystal structures. In addition, the width of the main APS line changes with thickness, which indicates changes of the local DOS.

As in the case of Fe on W(110), we measured the spin asymmetry of the main APS line as a function of the film thickness. The results are shown in figure 4 [8]. Below 2 ML, no asymmetry is observed. With increasing thickness, *A* for out-of-plane magnetization increases, passes a maximum and is strongly reduced between 5 and 10 ML, then it disappears. This is the thickness where the structural phase transition to bcc occurs and the magnetization changes to in-plane. The in-plane signal increases and saturates for thicker films. The three different structural and magnetic phases as described above are clearly seen in the APS spectra and corresponding asymmetry data. But there is more information. Compared with MOKE data in the literature, showing the magnetization signal between 5 and 10 ML to be almost constant [54, 58], the APS spin asymmetry decreases slightly with finite values different from zero. MOKE probes the magnetization of the Fe film averaged over the whole film thickness, APS only within the uppermost layers limited by the inelastic mean free path for 700 eV electrons in Fe. As a consequence, APS is able to distinguish between a magnetically live surface layer on non-ferromagnetic Fe and non-ferromagnetic Fe on top of a ferromagnetic Fe layer at the Fe/Cu interface. Model calculations for both scenarios are given in figure 4 as dashed and dash–dotted lines, respectively. Obviously, the APS results favour strongly the ferromagnetically live surface layer. This topic will be discussed in more detail in the following section.

As a function of the film thickness, the electronic structure develops from interface dominated to bulklike or, in cases where hybridization between substrate and overlayer states

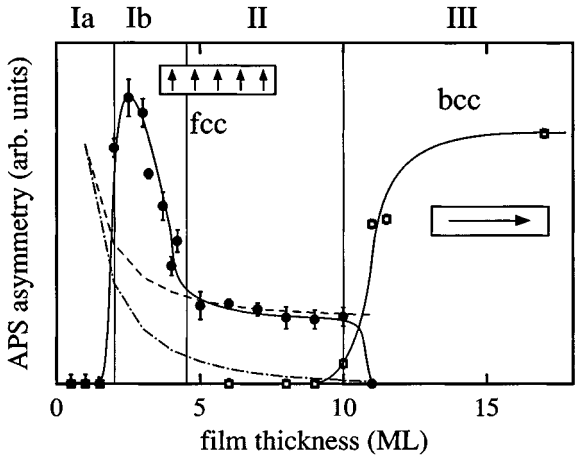

Figure 4. Spin asymmetry of the Fe $2p_{3/2}$ APS signal for Fe/Cu(001) as a function of the Fe film thickness taken at 100 K. Filled circles: magnetization along the surface normal. Open squares: magnetization in the surface plane. Dotted and dash–dotted lines: see text for details [8].

does not play a role, from two dimensional to three dimensional. The magnetic properties often deviate quite significantly from the bulk properties. Needless to note, in most thin-film systems structural changes occur as well, which complicate the analysis but often cause new interesting phenomena.

4. Depth dependence

Since thin-film systems are confined by a solid/solid and a solid/vacuum interface, an interesting question arises: are the magnetic properties uniform throughout the whole film or does a magnetic depth profile exist? Enhanced magnetic moments at surfaces have been predicted by theory and observed experimentally as discussed above. They are understood as consequences of band narrowing due to the reduced number of nearest neighbours at the surface. Surface Curie temperatures higher than bulk Curie temperatures have been reported for at least three systems: Gd/W(110) [63–66], $FeNi_3$(111) [67] and Tb/W(110) [68]. The results are controversially discussed in the literature and it is not clear to date which preparation conditions ensure that an enhanced surface Curie temperature is observed.

Fe/Cu(001), which was discussed in the preceding section, is a good example for a system with a magnetic depth profile. At film thicknesses between 5 and 10 ML, the magnetization, averaged over the whole film thickness, stays constant. The assumption of magnetically live surface layers was supported by adsorption experiments [54] but an unambiguous proof was lacking. Direct evidence of magnetically live surface layers was claimed to be found by site-selective conversion-electron Mössbauer spectroscopy [69] as well as magnetization-induced second-harmonic generation experiments [70]. The first approach suffers from measurement times of several days, which means contamination comes into play. The latter cannot *per se* distinguish between surface and interface.

In the following, it is shown that the analysis of electronic surface states and their spin dependence serves as a surface-layer-sensitive magnetic probe. The surface sensitivity depends only on the penetration depth of the wave function. Moreover, combined measurements of surface and bulk-derived states allow, to some extent, a depth-resolved study provided the

electronic structure is well understood. This is definitely the case for (001) surfaces with fcc crystal symmetry. The dispersion of d and sp-derived bulk states as well as image-potential and crystal-induced surface states is well documented and theoretically understood for a number of elements [71, 72]. As a consequence, the scene was set for spin-resolved IPE to tackle the Fe/Cu(001) problem. It has to be admitted, however, that the high surface sensitivity of IPE prevents access to the buried Fe/Cu interface.

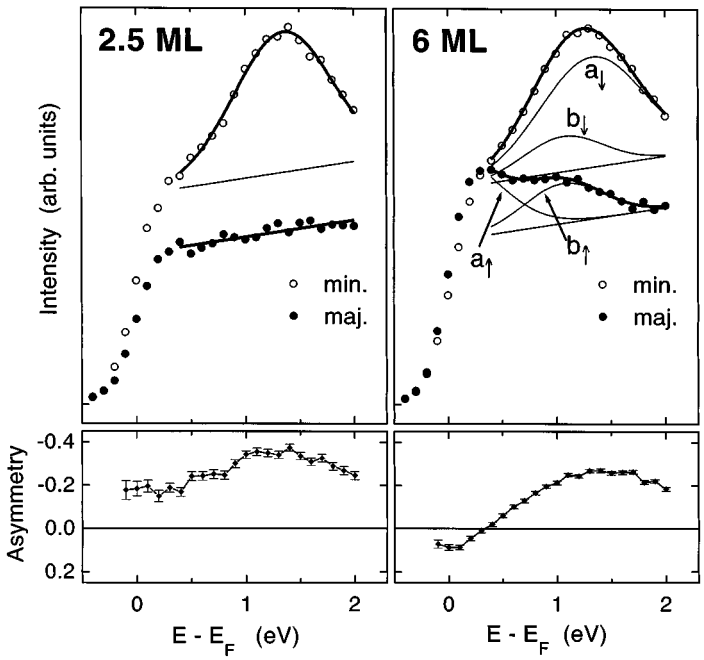

Figure 5. Spin-resolved IPE results and corresponding spin asymmetry for 2.5 and 6 ML of Fe on Cu(001). The data were taken at $T = 90$ K and at an electron incidence angle of 50°. Thick solid lines represent best fits to the data, thin solid lines the various fit components [10].

First, we focus our attention on direct transitions into an empty d band. Figure 5 shows spin-resolved IPE results together with the corresponding spin asymmetry for two film thicknesses, 2.5 and 6 ML of Fe on Cu(001), taken at an electron incidence angle of 50° [10]. In this geometry, our experiment is sensitive to the out-of-plane magnetization. (The angle of 40° between the electron spin polarization and the sample magnetization was taken into account when renormalizing the data to 100% hypothetical beam polarization.) 2.5 ML are known to be ferromagnetic throughout the film, while 6 ML exhibit the unusual reduced magnetization. For 2.5 ML, the spectra give evidence of a direct transition into a minority state with only background intensity in the majority channel. The spin asymmetry is minority dominated in the whole energy range shown. In contrast, the spectra for 6 ML show the minority feature somewhat shifted to lower energy and two features in the majority channel leading to a sign reversal in the asymmetry close to the Fermi energy. Surprisingly, the majority features appear at energies different from the minority feature. The results for 6 ML reflect the reduced magnetization and tell us about a more complicated electronic structure compared with 2.5 ML. A majority d band ($a_\uparrow$) shows up above the Fermi level, i.e. it becomes partially empty, which lowers the net spin density and, as a consequence, the magnetic moment. Combined with the small energetic downward shift of the minority emission ($a_\downarrow$), we conclude

that the magnetic exchange splitting $E_{a_\downarrow} - E_{a_\uparrow}$ of the d band under consideration, averaged over the ferromagnetic part of the film, is smaller for 6 ML than for the completely ferromagnetic 2.5 ML film. The extra emission b reflects the non-ferromagnetic part of the film, which is discussed in detail in the literature [10]. Without going into detail, the d-band emission of the 6 ML film gives evidence of the more complicated electronic structure with reduced magnetization compared with the 2.5 ML film.

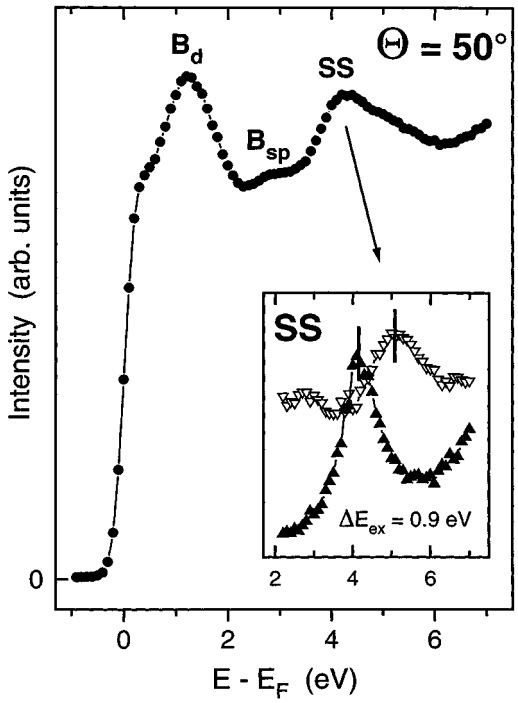

Figure 6. IPE results for 6 ML of Fe on Cu(001) taken at $T = 90$ K and at an electron incidence angle of 50°. The spin-averaged data are shown as an overview spectrum; spin-resolved data for the surface state SS are given in the inset in a limited energy interval. Open and filled triangles denote minority and majority spin, respectively [11].

To distinguish the surface layer and the layers underneath we tuned the experiment to a crystal-induced surface state. It is located in the middle of an energy gap in the projected bulk band structure, which guarantees a wave function which is peaked within the surface layer. Transitions into this surface state at $\bar{X}$ of the surface Brillouin zone at about 4.5 eV above the Fermi energy are induced by electrons with an angle of incidence of 50° relative to the surface normal. Figure 6 displays the spin-integrated spectrum and, in the energy range of the surface state, the spin-resolved intensities for 6 ML of Fe on Cu(001) (same sample condition as in the right panel of figure 5) [11]. The clear exchange splitting of the surface state SS of 0.9 eV is a direct and unique proof of a magnetically live surface layer in this system. A more comprehensive analysis of sp-derived bulk states and their exchange splitting (not given here) showed that the ferromagnetic order is not restricted to the topmost layer [11]. However, the size of the splitting in relation to the surface-state splitting indicates that the magnetic moment of the sublayers is reduced compared with the surface. These measurements demonstrate that a detailed study of the spin-dependent electronic structure can provide important information about a magnetic depth profile.

5. Temperature dependence

The most fundamental parameter in magnetism is the temperature. The long-range magnetic order decreases with increasing temperature and breaks down at a critical temperature called the Curie temperature. How this loss of long-range order occurs and how it is reflected in the spin-dependent electronic structure is a long-debated question. Since one knows from neutron scattering experiments that the local magnetic moments do not disappear at T_C, the degree of short-range magnetic order is another subject of discussion. Moreover, there is a difference depending on whether the magnetic moments are carried by the 3d conduction electrons in the case of band ferromagnets (Fe, Co, Ni) or by the localized 4f electrons in local-moment ferromagnets (Gd, Tb, ...). In the latter case, however, the local moments are indirectly coupled by again conduction electrons which itself carry some magnetic moment. In the literature much attention is given to the temperature dependence of the magnetization in two-dimensional films, which is described by the 2D Ising model or the 2D anisotropic Heisenberg model with their typical critical behaviour on approaching T_C [3, 6, 7].

In this paper, emphasis is given to the temperature dependence of the exchange splitting of electronic states. Delocalized states are expected to show a Stoner-like behaviour, i.e. the exchange splitting shrinks proportional to the magnetization and disappears at T_C. More localized states should keep their exchange splitting, only the experimental averaging over many local sites leads to a decrease of the spin asymmetry that vanishes at T_C owing to the loss of long-range magnetic order. In a spin-resolved experiment, this means a transfer of minority intensity into the majority channel and *vice versa*, often called spin mixing or extraordinary peaks in the literature. In real systems, depending on the degree of short-range magnetic order, all scenarios between the extrema 'Stoner-like' and 'spin mixing' are possible. While in Fe evidence was found for extraordinary peaks indicative of short-range magnetic order [73, 74], the situation for Ni is not as clear. PE and IPE experiments found collapsing band behaviour with line broadening [75, 76, 38], while the results of two other techniques favour an almost constant exchange splitting: spin-polarized electron-energy-loss spectroscopy [77] and two-dimensional angular correlation of (polarized positron) annihilation radiation [78]. In addition, results of spin-resolved resonant PE were well explained by the existence of a temperature-independent local magnetization which fluctuates at elevated temperatures [79]. Spin-resolved circularly polarized resonant PE even found local spin polarization of the 3d bands, not only below but also above the Curie temperature [80]. The theoretical description is not complete either [81–83].

Gd on W(110) remains a hot topic in thin-film magnetism because of the unusual surface magnetic properties reported for this system [65, 66]. In particular, a d_{z^2}-type surface state is expected to be responsible or at least influence the surface magnetic behaviour like an enhanced Curie temperature and/or a canted spin structure compared with the sublayers. PE and IPE, both spin integrated and spin resolved, as well as scanning tunnelling spectroscopy (STS) have been employed to learn more about this surface state and its temperature behaviour. It was hoped that a comparison between the temperature dependence of bulk and surface states could also reveal the degree of localization of the surface state. The surface state is magnetically relevant because it is partially occupied with different occupation in the two spin channels, which means it contributes directly to the magnetic moment of the surface. Theory expects a majority state below and a minority state above the Fermi level for zero temperature [84]. At low temperatures, the two components were experimentally observed, separated in energy by about 0.7 eV, but the spin character was not purely majority below E_F and not purely minority above E_F [85, 14, 86]. The temperature-dependent results were interpreted controversially as spin-mixing or collapsing-band behaviour or in between with a remaining splitting of 0.4 eV

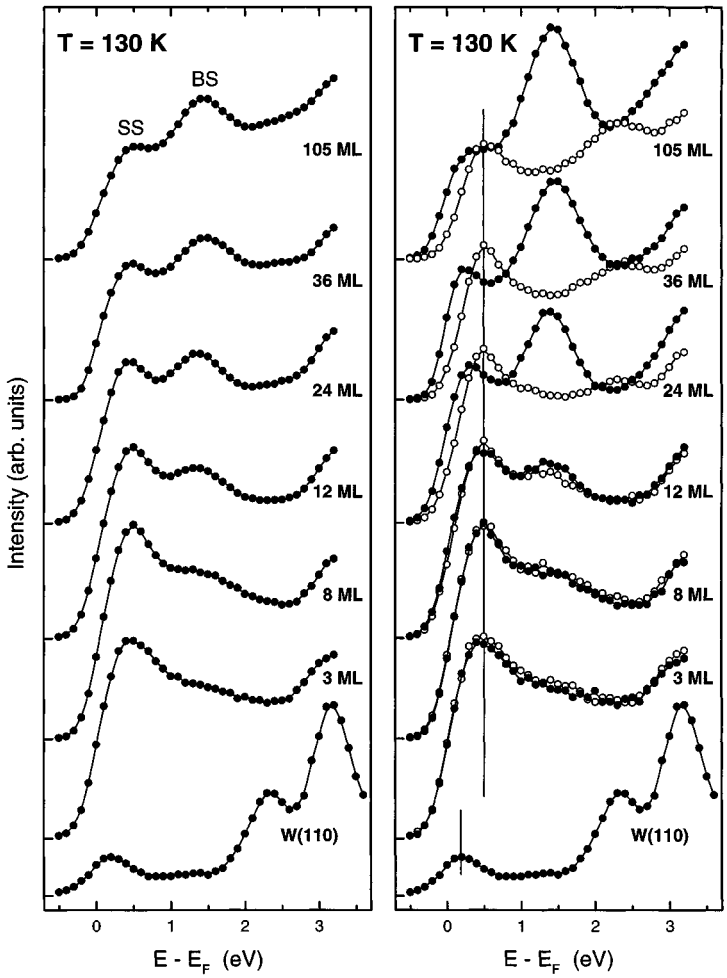

Figure 7. Spin-averaged (left panel) and spin-resolved (right panel) IPE spectra for Gd films on W(110) for various overlayer thicknesses taken at $T = 130$ K and normal electron incidence. Open and filled dots (right panel) denote minority and majority spin, respectively. The intensity of the W(110) spectrum is not plotted to scale [15].

at T_C [85, 87, 14, 88]. Each individual technique has its strengths and its constraints but none of them was able to provide a complete picture. The results of PE and IPE are distorted by the Fermi level cutoff in combination with a limited energy resolution, while STS has no or limited spin resolution. This explains the diverging interpretations.

Figure 7 shows spin-integrated and spin-resolved IPE data for Gd/W(110) taken at $T = 130$ K for normal electron incidence for different coverages [15]. Due to the extremely short probing depth in Gd of about 1 ML, the spectra for 3 ML no longer show any substrate signal. This also proves that there are no holes in the film. The spin-integrated spectra reveal the surface-state emission SS just above the Fermi level and transitions into d-like bulk states BS at about 1.4 eV. The spin-resolved data exhibit pronounced spin asymmetry only for the thicker films, although the Curie temperatures for 8 and 12 ML thick films are well above the measurement temperature of 130 K [89] and the peak positions of SS and BS also

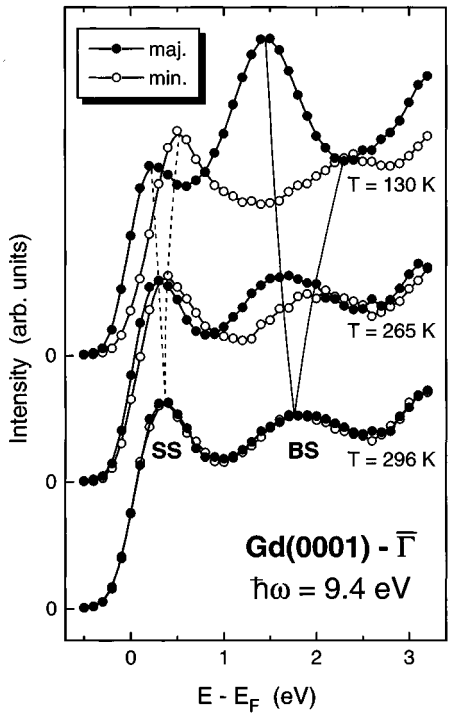

Figure 8. Spin-resolved IPE spectra for normal electron incidence on a 36 ML thick Gd(0001) film on W(110) for three different temperatures [14].

indicate ferromagnetic order [15]. It is not clear at present why we do not observe clear spin dependences. The most probable hypothesis is a changed magnetic anisotropy for thin films, which prevents a remanent magnetization in the direction of the spin polarization of the exciting electrons. Experiments are under way to clarify this question. The spectra for thicker films show clearly two spin components for both BS and SS, which are energetically separated by 0.85 and 0.25 eV, respectively. The intensity imbalance between the two spin components of BS is remarkable. This can be explained by a spin dependence of the attenuation length of the incident electrons. If this is true, the effect should be absent for SS. In fact, SS has even a reversed intensity ratio between minority and majority components. The somewhat lower intensity of the majority component is a consequence of the Fermi level cutoff or of a smaller spectral density.

Figure 8 presents spin-resolved IPE data for 36 ML of Gd on W(110) taken at three different temperatures that correspond to about 90, 45 and 0% of the spontaneous bulk magnetization at $T = 0$ [14]. For 36 ML thick films T_C is reported to be a few Kelvin below the bulk value [89], in agreement with our MOKE measurements. BS shows a Stoner-like temperature behaviour accompanied by a broadening of the observed features. In addition, the spin dependence of the peak intensities disappears upon approaching the Curie temperature. As expected, the electron attenuation length is no longer spin dependent at T_C. For SS, the two unoccupied spin components move towards each other with increasing temperature, forming one spin-independent spectral feature at about the bulk Curie temperature. The temperature behaviour of SS is again Stoner-like with broadening effects. We did not find evidence of an enhanced surface T_C.

In the light of the PE results with a primarily majority surface state below E_F the observation of a majority-spin component of SS above the Fermi energy is surprising. Moreover, the collapsing-band behaviour of the unoccupied part of SS is unexpected with the STS data in mind, which see clear features below and above E_F at and above T_C. The interpretations given in the literature seem to be biased by the assumption that there is only one minority and one majority component, which then show either spin-mixing or collapsing-band behaviour. Probably the situation is more complicated. The strong localization of the surface state may lead to considerable f–d interaction, which is believed to be responsible for the main energetic splitting of 0.7 eV between the occupied and the unoccupied components. Each component exhibits a spin dependence, at least in the unoccupied part accompanied by a spin splitting. At the Curie temperature, the spin dependences and spin splittings disappear. Both spectral densities, the occupied and the unoccupied, are somewhat shifted towards the Fermi level, but an energetic splitting of 0.4 eV remains at T_C. Model calculations support this scenario [90, 91].

The described example of Gd films on W(110) demonstrates the complexity of the temperature-dependent electronic structure in ferromagnets, whether films or bulk materials. It is far from being well understood. The combined results from various techniques and intense discussions between the researchers who obtained the results promise an increased microscopic understanding of the fascinating phenomenon 'collective magnetism'.

6. Conclusions

The magnetic order in ultrathin films differs in many aspects from the bulk properties. It depends critically on the film thickness including the growth mode and structural changes. In addition, a magnetic depth profile may develop influenced by the particular interfaces, the substrate on the one side and the vacuum or overlayer on the other side, and the magnetic order depends on the temperature, which is the most fundamental parameter in magnetism. All this makes thin-film systems attractive to both basic and applied research. To describe the magnetic properties on a microscopic level needs the understanding of the underlying spin-dependent electronic structure. In this paper, spin-resolved appearance potential spectroscopy and inverse photoemission were used to determine the spin dependence of the unoccupied states in magnetic thin-film systems. While the first gives access to the local density of states, the latter provides $\boldsymbol{k}$-resolved information about specific states characteristic of the surface or the layers underneath. Examples of Fe and Gd films were discussed in this paper.

The direct correlation between magnetic order and electronic structure, i.e. an *in situ* measurement of both, is essential, particularly in thin-film systems, where the properties depend critically on the preparation parameters. Usually the 'macroscopic' magnetic order is checked by MOKE. However, the probing depth of MOKE is orders of magnitude larger than the probing depth of spin-resolved electron spectroscopies, which hampers a direct comparison. Therefore, we included an additional technique in our system recently, spin-polarized secondary electron emission, for magnetometry [2, 92]. This allows us now to probe the magnetic order and the electronic states of the same sample with approximately the same probing depth.

Acknowledgments

I wish to express my gratitude to V Dose for continuous support. It is a pleasure to thank Th Detzel, B Gubanka, H D Kang, Ch Math, G Rangelov and J Reinmuth for their enjoyable collaboration and M Bode, P A Dowben, H Ebert, M Farle and W Nolting for

helpful discussions. Financial support from the Deutsche Forschungsgemeinschaft is gratefully acknowledged.

References

[1] Cullity B D 1972 *Introduction to Magnetic Materials* (Reading, MA: Addison-Wesley)
[2] Siegmann H C 1992 *J. Phys.: Condens. Matter* **4** 8395
[3] Gradmann U 1993 *Handbook of Magnetic Materials* vol 7, ed K H J Buschow (Amsterdam: Elsevier) p 1
[4] Farrow R F C, Dieny B, Donath N, Fert A and Hermsmeier B D (eds) 1993 *Magnetism and Structure in Systems of Reduced Dimension* (New York: Plenum)
[5] Bland J A C and Heinrich B (eds) 1994 *Ultrathin Magnetic Stuctures I* (Berlin: Springer)
Heinrich B and Bland J A C (eds) *Ultrathin Magnetic Structures II* (Berlin: Springer)
[6] Allenspach R 1994 *J. Magn. Magn. Mater.* **129** 160
[7] Elmers H J 1995 *Int. J. Mod. Phys.* B **9** 3115
[8] Detzel Th, Vonbank M, Donath M and Dose V 1995 *J. Magn. Magn. Mater.* **147** L1
Detzel Th, Memmel N, Vonbank M, Donath M and Dose V 1995 *Phys. Low-Dimens. Struct.* **8–9** 1
[9] Detzel Th, Vonbank M, Donath M, Memmel N and Dose V 1996 *J. Magn. Magn. Mater.* **152** 287
[10] Gubanka B, Donath M and Passek F 1996 *J. Magn. Magn. Mater.* **161** L11
[11] Gubanka B, Donath M and Passek F 1996 *Phys. Rev.* B **54** R11 153
[12] Passek F, Donath M and Ertl K 1996 *J. Magn. Magn. Mater.* **159** 103
[13] Rangelov G, Kang H D, Reinmuth J and Donath M 1999 *Phys. Rev.* B, at press
[14] Donath M, Gubanka B and Passek F 1996 *Phys. Rev. Lett.* **77** 5138
[15] Donath M and Gubanka B 1998 *Magnetism and Electronic Correlations in Local-Moment Systems: Rare-Earth Elements and Compounds* ed M Donath, P A Dowben and W Nolting (Singapore: World Scientific) p 217
[16] Aspelmeier A, Gerhardter F and Baberschke K 1994 *J. Magn. Magn. Mater.* **132** 22
[17] Kolac U, Donath M, Ertl K, Liebl H and Dose V 1988 *Rev. Sci. Instrum.* **59** 1933
[18] Donath M 1989 *Appl. Phys.* A **49** 351
[19] von der Linden W, Donath M and Dose V 1993 *Phys. Rev. Lett.* **71** 899
[20] Rangelov G, Ertl K, Passek F, Vonbank M, Bassen S, Reinmuth J, Donath M and Dose V 1998 *J. Vac. Sci. Technol.* A **16** 2738
[21] Thomas Ch H 1925 *Phys. Rev.* **25** 322
[22] Park R L and Houston J E 1972 *Phys. Rev.* B **6** 1073
[23] Park R L 1975 *Surf. Sci.* **48** 80
[24] Dose V and Reusing G 1983 *Solid State Commun.* **48** 683
[25] Powell C J, Erickson N E and Ramaker D E 1992 *Phys. Scr.* **T41** 175
[26] Giber J, Drube R and Dose V 1991 *Appl. Phys.* A **52** 167
[27] Dose V, Drube R and Hrtl A 1986 *Solid State Commun.* **57** 273
[28] Reinmuth J, Passek F, Petrov V N, Donath M, Popescu V and Ebert H 1997 *Phys. Rev.* B **56** 12 893
[29] Kirschner J 1984 *Solid State Commun.* **49** 39
[30] Ertl K, Vonbank M, Dose V and Noffke J 1993 *Solid State Commun.* **88** 557
[31] Kang H, Rangelov G, Reinmuth J and Donath M 1999 *Surf. Sci.* submitted
[32] Ebert H and Popescu V 1997 *Phys. Rev.* B **56** 12884
[33] Reinmuth J, Donath M, Passek F and Petrov V N 1998 *J. Phys.: Condens. Matter* **10** 4027
[34] Dose V 1985 *Surf. Sci. Rep.* **5** 337
[35] Smith N V 1988 *Rep. Prog. Phys.* **51** 1227
[36] Dose V, Fauster Th and Schneider R 1986 *Appl. Phys.* A **40** 203
[37] Donath M 1993 *Magnetism and Structure in Systems of Reduced Dimension* ed R F C Farrow, B Dieny, M Donath, A Fert and B D Hermsmeier (New York: Plenum) p 243
[38] Donath M 1994 *Surf. Sci. Rep.* **20** 251
[39] Pappas D P, Kämper K-P, Miller B P, Hopster H, Fowler D E, Brundle C R, Luntz A C and Shen Z-X 1991 *Phys. Rev. Lett.* **66** 504
[40] Siegmann H C 1994 *Surf. Sci.* **307–9** 1076
[41] Donath M 1995 *Electronic Surface and Interface States on Metallic Systems* ed E Bertel and M Donath (Singapore: World Scientific) p 233
[42] Gradmann U and Waller G 1982 *Surf. Sci.* **116** 539
[43] Gardiner T M 1983 *Thin Solid Films* **105** 213
[44] Elmers H J and Gradmann U 1990 *Appl. Phys.* A **51** 255

[45] Bethge H, Heuer D, Jensen Ch, Reshöft K and Köhler U 1995 *Surf. Sci.* **331–3** 878
[46] Gradmann U, Korecki J and Waller G 1986 *Appl. Phys.* A **39** 101
[47] Elmers H J, Hauschild J, Fritsche H, Liu G, Gradmann U and Köhler U 1995 *Phys. Rev. Lett.* **75** 2031
[48] Sander D, Skomski R, Schmidthals, Enders A and Kirschner J 1996 *Phys. Rev. Lett.* **77** 2566
[49] Ohnishi S, Weinert M and Freeman A J 1984 *Phys. Rev.* B **30** 36
[50] Victora R H and Falicov L M 1985 *Phys. Rev.* B **31** 7335
[51] Waller G and Gradmann U 1982 *Phys. Rev.* B **26** 6330
[52] Tamura E, Feder R, Waller G and Gradmann U 1990 *Phys. Status Solidi* b **157** 627
[53] Albrecht M, Gradmann U, Furubayashi T and Harrison W A 1992 *Europhys. Lett.* **20** 65
[54] Thomassen J, May F, Feldmann B, Wuttig M and Ibach H 1992 *Phys. Rev. Lett.* **69** 3831
[55] Bayer P, Müller S, Schmailzl P and Heinz K 1993 *Phys. Rev.* **48** 17 611
[56] Kalki K, Chambliss D D, Johnson K E, Wilson R J and Chiang S 1993 *Phys. Rev.* **48** 18 344
[57] Li Donqi, Freitag M, Pearson J, Qui Z Q and Bader S D 1994 *Phys. Rev. Lett.* **72** 3112
[58] Mueller S, Bayer P, Reischl C, Heinz K, Feldmann B, Zillgen H and Wuttig M 1995 *Phys. Rev. Lett.* **74** 765
[59] Ellerbrock R D, Fuest A, Schatz A, Keune W and Brand R A 1995 *Phys. Rev. Lett.* **74** 3053
[60] Zharnikov M, Dittschar A, Kuch W, Schneider C M and Kirschner J 1996 *Phys. Rev. Lett.* **76** 4620
[61] Platow W, Farle M and Baberschke K 1998 *Europhys. Lett.* **43** 713
[62] Härtl A 1985 *Dissertation* Universität Würzburg
[63] Weller D, Alvarado S F, Gudat W, Schröder K and Campagna M 1985 *Phys. Rev. Lett.* **54** 1555
[64] Rau C and Eichner S *Phys. Rev.* B **34** 6347
[65] Dowben P A, McIlroy D N and Li Donqi 1997 *Handbook on the Physics and Chemistry of Rare Earths* vol 24, ed K A Gschneidner Jr and L Eyring (Amsterdam: Elsevier) ch 159
[66] Donath M, Dowben P A and Nolting W (eds) 1998 *Magnetism and Electronic correlations in Local-Moment Systems: Rare-Earth Elements and Compounds* (Singapore: World Scientific)
[67] Mamaev Yu A, Petrov V N and Starovoitov S A 1987 *Sov. Tech. Phys. Lett.* **13** 642
[68] Rau C and Jin C 1988 *J. Physique Coll.* **12** C8 1627
Rau C 1989 *Appl. Phys.* A **49** 579
[69] Keune W, Schatz A, Ellerbrock R D, Fuest A, Wilmers K and Brand R A 1996 *J. Appl. Phys.* **79** 4265
[70] Straub M, Vollmer R and Kirschner J 1996 *Phys. Rev. Lett.* **77** 743
[71] Landolt–Bönstein New Series 1994 Group III, vol 24, part b (Berlin: Springer) p 29
[72] Goldmann A, Dose V and Borstel G 1985 *Phys. Rev.* B **32** 1971
[73] Kisker E, Schröder K, Campagna M and Gudat W 1984 *Phys. Rev. Lett.* **52** 2285
Kisker E, Schröder K, Gudat W and Campagna M 1985 *Phys. Rev.* B **31** 329
[74] Clauberg R, Haines E M and Feder R 1985 *Z. Phys.* **62** 31
[75] Hopster H, Raue R, Güntherodt G, Kisker E, Clauberg R and Campagna M 1983 *Phys. Rev. Lett.* **51** 829
[76] Donath M and Dose V 1989 *Europhys. Lett.* **9** 821
[77] Kirshner J and Langenbach E 1988 *Solid State Commun.* **66** 761
[78] Genoud P, Manuel A A, Walker E and Peter M 1991 *J. Phys.: Condens. Matter* **3** 4201
[79] Kakizaki A, Fujii K, Shimada K, Kamata A, Ono K, Park K-H, Kinoshita T, Ishii T and Fukutani H 1994 *Phys. Rev. Lett.* **72** 2781
[80] Sinkovic B, Tjeng L H, Brookes N B, Goedkoop J B, Hesper R, Pellegrin E, de Groot F M F, Altieri S, Hulbert S L, Shekel E and Sawatzky G A 1997 *Phys. Rev. Lett.* **79** 3510
[81] Capellmann H (ed) 1987 *Metallic Magnetism (Topics in Current Physics 42)* (Berlin: Springer)
[82] Nolting W, Borgiel W, Dose V and Fauster Th 1989 *Phys. Rev.* B **40** 5015
Nolting W, Vega A and Fauster Th 1994 *Z. Phys.* B **96** 357
[83] Uhl M and Kübler J 1996 *Phys. Rev. Lett.* **77** 334
[84] Wu R and Freeman A J 1991 *J. Magn. Magn. Mater.* **99** 81
[85] Li Donqi, Pearson J, Bader S D, McIlroy D N, Waldried C and Dowben P A 1995 *Phys. Rev.* B **51** 13895
[86] Fedorov A V, Valla T, Huang D J, Reisfeld G, Loeb F, Liu F and Johnson P D 1998 *J. Electron Spectrosc. Relat. Phenom.* **92** 19
[87] Weschke E, Schlüssler-Langeheine C, Meier R, Fedorov A V, Starke K, Hübinger F and Kaindl G 1996 *Phys. Rev. Lett.* **77** 3415
[88] Getzlaff M, Bode M, Heinze S, Pascal R and Wiesendanger R 1998 *J. Magn. Magn. Mater.* **184** 155
[89] Farle M, Baberschke K, Stetter U, Aspelmeier A and Gerhardter F 1993 *Phys. Rev.* B **47** 11 571
[90] Nolting W and Matlak M 1984 *Phys. Status Solidi* b **123** 155
[91] Nolting W, Dambeck T and Borstel G 1994 *Z. Phys.* B **94** 409
[92] Donath M 1993 *Surf. Sci.* **287–8** 722